COMPOSITION AND IMPACT DEFORMATION OF NOACHIAN BASEMENT WEST OF ISIDIS E. L. Scheller[1] and B. L. Ehlmann[1,2], [1]Division of Geological and Planetary Sciences, California Institute of Technology, Pasadena, CA, USA [2]Jet Propulsion Laboratory, California Institute of Technology, Pasadena, CA, USA (eschelle@caltech.edu).

Introduction: The Noachian basement of the NE Syrtis/Nili Fossae region provides constraints on the origin and evolution of the oldest Martian crust. The Noachian basement is composed of low-Ca pyroxene (LCP), Fe/Mg-smectites, and Al-phillosilicates[1-3] with evidence of extensive aqueous alteration.[3-7] The Early- or Mid-Noachian[8-10] Isidis impact caused widespread brecciation and deformation of pre-existing crust to form the observed Noachian basement[1,3,11-12] obscuring primary geological features of the basement. This study assesses the extent and nature of impact deformation in the basement to determine the composition, structure, and geological history of the Noachian basement, including discernment of pre-impact structure, if possible. The Noachian basement and megabreccia blocks accessible in the NE Syrtis landing site ellipse and nearby region are of high importance for the future landing site selection of the Mars 2020 rover mission. Understanding the Noachian basement can constrain Martian crust composition as well as the surface and subsurface environments during the earliest part of Maritan history. Additionally, the Isidis basin provides insight into the effects of basin-scale impact processes, a key geologic process throughout the solar system.

Mapping of megabreccia: We mapped 147 megabreccia exposures in the regional area west of Isidis basin (covering Nili Fossae, NE Syrtis, and the Jezero Watershed (Fig. 1). Megabreccia blocks span a size range of <1 m to several hundreds of meters. Hence, the resolution of CTX (6 m/pixel)[13] and CRISM (18 m/pixel)[14] allow observation of certain megabreccia blocks, but it is the spatial resolution and coverage area of HiRISE (0.25-1.3 m/pixel)[15] data that controls the observed distribution of megabreccia. We also searched southern and eastern rim segments of Isidis basin. No megabreccia exposures were observed, though HiRISE data coverage is comparatively sparse.

From our mapping, we suggest five initial classifications of megabreccia exposures on the basis of textural differences (Fig. 2). First, we attribute the terms ***densely packed blocks (DP)*** to blocks that are in contact with each other, ***scattered blocks (SC)*** to blocks that are not in contact with each other, and ***single blocks (SI)*** to blocks that appear with no association to larger exposures. Second, DP blocks can appear monomict ***(MDP)*** or polymict ***(PDP)***, depending on the number of distinct lithologies present. Third, certain PDP blocks exhibit layering ***(LDP)*** with meter to tens of meter scale banding of material with alternating colors and albedo.

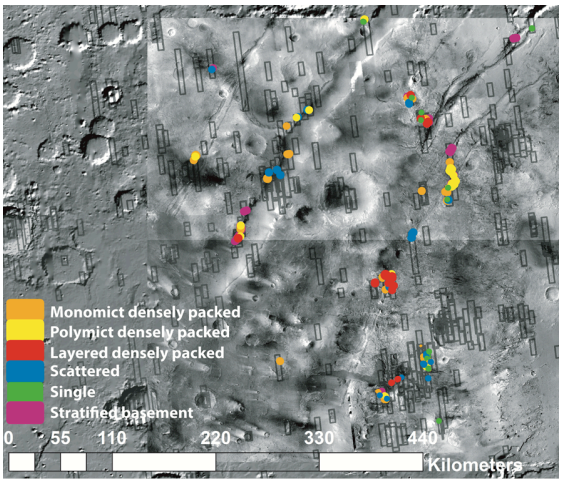

Figure 1: Preliminary map of the distribution of megabreccia textures over the study area. HiRISE coverage outlined in black.

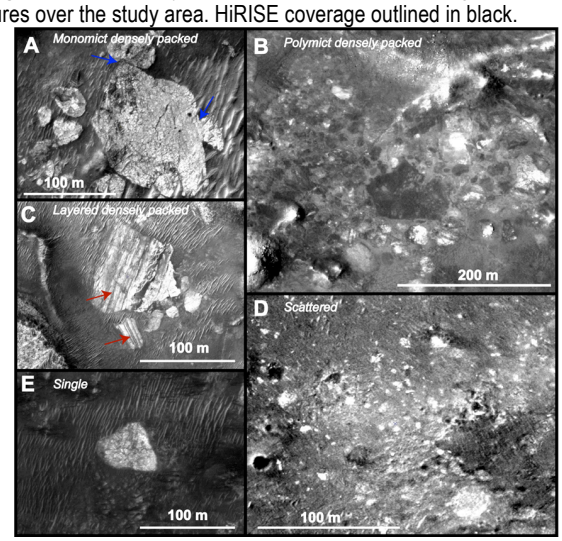

Figure 2: Examples of different textures of megabreccia. (A) Monomict densely packed blocks (MDP) (ESP_033572_1995). (B) Polymict densely packed blocks (PDP) (ESP_037185_2010). (C) Layered densely packed blocks (LDP) show banding of darker and brighter albedo material, as indicated with red arrows (ESP_035062_1995). (D) Scattered block exposures (SC) (PSP_008861_2000). (E) Single block (SI) example (ESP_046271_1980).

Basement stratification: In select locales, basement materials exhibit banding over hundreds of meters to multiple kilometers (Fig. 2). Wall-exposures of stratified basement in the Nili Fossae reveal faults and possible fold structures that disrupt the horizontal layering. Compositionally, layers consist primarily of Fe/Mg-smectite, although LCP layers have been observed as well.[1]

Composition of megabreccia: Eleven exposures in 7 different CRISM images contain blocks larger than a CRISM pixel. Spectra were taken for single blocks but also averaged over several blocks with similar composition as inferred from HiRISE color (as in [1]).[16] All spectra were ratioed to spectrally bland units in the same column and/or treated with a noise reducing algorithm[17]. Tornabene et al. (2013) previously correlated Isidis megabreccia blocks to Fe/Mg-smectites.[12] In this study, 4 exposures contained blocks of exclusively Fe/Mg-smectite composition, while 2 exposures contained blocks of exclusively LCP and Fe/Mg-smectite mixture composition. The last 5 exposures contained blocks variably composed of Fe/Mg-smectite and LCP-Fe/Mg-smectite mixtures. Additionally, we used color HiRISE data to examine the composition of additional megabreccia exposures[16], mapping blocks of mafic (LCP) compositions with high BG/RED and BG/IR ratioes[18] versus altered compositions with high IR/BG and IR/RED ratios.[18]

Composition of the basement: Initial results from 34 CRISM images and a regional CTX DEM suggest a topographic dependency in composition. Basement in depressions or slopes consist primarily of Fe/Mg-smectites), while elevated plains consist primarily of LCP. Wall exposures of basement in depressions, grabens, and fluvially incised canyons often show a sharp contact between stratigraphically lower Fe/Mg-smectite and overlying LCP, although examples with reversed stratigraphic order do occur. Additionally, topographic highs in the form of eroded basement mounds composed of Fe/Mg-smectite occur in the otherwise smooth LCP-dominated plains.[5] The raised linear ridges structures[1,6,7] of the Noachian basement are also associated primarily with Fe/Mg-smectite spectral signature.

Stratigraphic relationships: The mottled and fractured olivine- and carbonate-bearing unit[1-5,11] and younger impact melts noticeably overlie megabreccia blocks throughout the mapped area. The raised linear ridges structures cross-cut layers of stratified basement and megabreccia blocks. Fig. 3 summarizes our current understanding of the geological timeline of the Noachian basement unit. The pre-impact LCP-bearing basement underwent an episode of aqueous alteration that included formation of Fe/Mg-smectite.[1,3] The exact processes and timing leading to formation of LCP, phyllosilicates, and basement stratification are currently being investigated, but there do appear to be two pre-impact altered crust types: massive and stratified. Brecciation and deformation by the Isidis impact occurred after the alteration. Then, raised linear ridges composed of primarily alteration mineralogies cross-cut the impact deformed basement. The formation of kaolinite occurs patchily throughout the basement in both LCP and Fe/Mg-dominated parts as patches, mounds, and layers. Breccia blocks do not appear to contain kaolinite. Hence, it is possible that the kaolinite represent a later surface weathering event[3] but the low spatial extent of kaolinite must be taken into account as well.

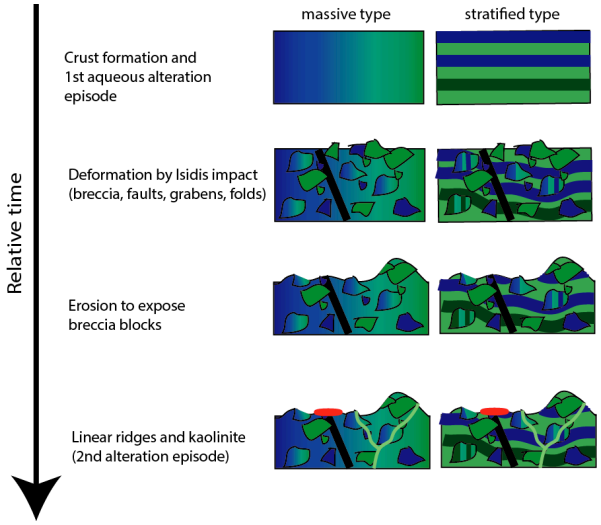

Figure 1: Preliminary timeline of processes forming the Noachian basement west of Isidis (Blue=LCP; Green=Fe/Mg-smectite; Red= kaolinite). Pre-Isidis stages involve aqueous alteration and stratification. Post-Isidis stages involve at least two episodes of aqueous alteration, forming linear ridges and kaolinite, respectively.

Conclusions and future work: Our mapping of megabreccia west of Isidis reveals multiple textures that serve as indicators of stratigraphic relationships within the Noachian basement. Layered densely packed (LDP) blocks and stratified basement may be related to brittle (and possibly plastic) deformation during the Isidis impact. These are large sections of early or Pre-Noachian strata that pre-date the earliest surfaces and are available for in situ study. The linear ridges of the Noachian basement represent a secondary alteration episode postdating deformation by the Isidis impact. Future efforts will assess the presence or absence of spectral variability in the Fe/Mg smectite and mafic portions of the basement, the origin of their present topographic relationships, structural analysis of possible folds, and stratigraphic relationships between alteration and mafic lithologies.

Acknowledgements: Thanks to B. Weiss, N. Lanza, H. Newsom, Z. Gallegos, and the M2020 team for discussion.

References: [1] Mustard J. F. et al. (2009) *JGR, 114* (E2). [2] Ehlmann, B. L. and Mustard, J.F. (2012) *GRL, 39* 11. [3] Ehlmann, B. L. et al. (2009), *JGR, 114* (E2). [4] Goudge, T. A. et al. (2015), *JGR, 120,* 775-808. [5] Mangold, N. et al. (2017) *JGR, 112,* E8. [6] Saper, L. and Mustard, J.F. (2013) *GRL, 40,* 245-249. [7] Pascuzzo, A.C. and Mustard, J.F. (2017) *LPSC XLVIII*. [8] Werner, S. C. et al. (2008) *Icarus, 195,* 45-60. [9] Frey, H. et al. (2008) *GRL, 35* (13). [10] Fassett, C. I. and Head, J. W. (2011) *Icarus, 211,* 1204-1214. [11] Bramble, M. S., et al. (2017), *Icarus, 293,* 66-93. [12] Tornabene, L. L. et al. (2013) *JGR, 118,* 994-1012. [13] Malin, M. C. et al. (2007) *JGR, 112* (E5). [14] Murchie, S. et al. (2007) *JGR, 112* (E5). [15] McEwen, A. S. et al. (2007) *JGR, 112* (E5). [16] Weiss, B. et al. (2018) *LPSC XLIX*. [17] Pan, L. et al. (2017) *JGR, 122,* 1824-1854. [18] Delamere, W. A. et al. (2010) *Icarus, 205,* 38-52.